CHEMISTRY OF MATERIALS

ARTICLE

pubs.acs.org/cm

A New Family of Fast Sodium Ion Conductors: $Na_2M_2TeO_6$ (M = Ni, Co, Zn, Mg)

Maria A. Evstigneeva,* Vladimir B. Nalbandyan, Aleksandr A. Petrenko, Boris S. Medvedev, and Aleksandr A. Kataev

Southern Federal University, 7 ul. Zorge, Rostov-na-Donu, 344090 Russia

Supporting Information

ABSTRACT: The four compounds $Na_2M_2TeO_6$ (M^{2+} = Ni, Co, Zn, Mg) have been prepared by solid-state reactions in air at 600−820 °C and characterized by powder X-ray diffraction, redox titration, impedance, and polarization measurements on ceramic samples. All of them are superstructures of the well-known hexagonal layered P2-type with ordering of M and Te in octahedral brucite-like layers. They have similar parameters of the hexagonal cells: a = 5.20−5.28 Å, c = 11.14−11.31 Å, but different stacking sequences along c. With M = Co, Zn, Mg ($P6_322$), there are columns Te M Te M and M M M M, but with M = Ni ($P6_3/mcm$), there are columns Te Te Te Te and Ni Ni Ni Ni. As little as 5% Li substitution for Ni induces transformation to the $P6_322$ structure. Sodium ions in the interlayer gaps are disordered over a number of trigonal prisms sharing faces and exhibit high conductivity: 4−11 S/m at 300 °C, despite relatively low densities of the ceramics. The materials are purely ionic conductors; the largest electronic contribution (0.1% at 300 °C) has been found for the Co compound, presumably due to a minor admixture of Co(3+).

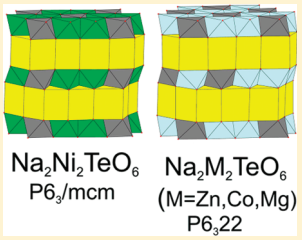

KEYWORDS: tellurate, ion conduction, Rietveld, superlattice, layered structure

1. INTRODUCTION

A family of hexagonal layered P2-type phases is noticed not only for their thermoelectric properties[1,2] and superconductivity[3,4] of sodium cobalt bronzes Na_xCoO_2 or hydrates and for ion-exchange preparation of Li-ion battery materials[5,6] but also for their excellent alkali ion conduction properties. Alkali ions are distributed over a number of trigonal prisms sharing their rectangular faces and thus providing wide passages for cation transport; electronic conduction is suppressed when all the components are in their stable oxidation states. Examples are $K_x(In_xM^{4+}_{1-x})O_2$ (M = Sn, Zr, Hf, Pb),[7] $K_x(M^{2+}_{x/2}Sn_{1-x/2})O_2$ (M = Zn, Mg, Ca),[8] $K_x(M^{2+}_{(1+x)/3}Sb_{(2-x)/3})O_2$ (M = Ni, Co, Mg),[9] $Na_xM^{2+}_{x/2}Ti^{4+}_{1-x/2}O_2$ (M = Ni, Co),[10,11] $Na_xCr^{3+}_xTi^{4+}_{1-x}O_2$,[12] and $Na_xLi^{+}_{x/3}Ti^{4+}_{1-x/3}O_2$.[13]

All of them are intrinsically nonstoichiometric. Their homogeneity ranges do not include x = 1, and the neutron[6,14] and X-ray[7−9,13] diffraction data indicate that heterovalent octahedral cations (e.g., Ni^{2+} and Ti^{4+}, Ni^{2+} and Sb^{5+}, Li^{+} and Ti^{4+}, etc.) remain disordered on a unique crystallographic Wyckoff position even when their ratio approaches "stoichiometric" values of 1:1, 1:2, or 1:3. It seemed for a long time that disordered arrangement of alkali cations and their high mobility are due to this disorder in the rigid lattice (established at high preparation temperatures and quenched to the room temperature), and with heterovalent cations ordered, the condition of local electroneutrality would lead to corresponding alkali/vacancy ordering and lowering of the conductivity. This idea received confirmation when a series of alkali/vacancy ordered Na_xCoO_2 and K_xCoO_2 superstructures[15−19] were discovered. All octahedra are occupied there by the same element, and thus, charge ordering within the brucite-like layers may be achieved easily even at low temperatures,[13] in contrast to the solid electrolytes listed above, where diffusion of heterovalent elements is needed.

In this paper, however, we report a new group of P2-type phases $Na_2M_2TeO_6$ (x = 2/3) that are stoichiometric, ordered, and still exhibit high sodium ion conductivities. Their synthesis was stimulated by the report on a structurally related (O3-derived) $Na_2Cu_2TeO_6$ phase.[20] We suggested that other divalent cations substituting for Cu may give rise to P2-derived polytypes, and this was confirmed experimentally.

Indexed powder patterns of $Na_2M_2TeO_6$, with M = Zn and Ni, were submitted to the Powder Diffraction File in 2006 (PDF # 00-58-0051 and 00-58-0052). Some preliminary results were reported in brief elsewhere.[21,22] When this work was in progress, a paper appeared describing preparation and powder neutron diffraction investigation of $Na_2Co_2TeO_6$.[23] Those authors were interested in magnetic properties and did not study conductivity. We discuss below their structural results along with ours.

2. EXPERIMENTAL SECTION

Samples with the general formula $Na_xM^{2+}_{(2+x)/4}Te^{6+}_{(2-x)/4}O_2$ (M = Ni, Co, Zn, Mg) were prepared by conventional solid-state reactions. Starting materials were reagent-grade sodium carbonate, sodium nitrate, tellurium dioxide, hydrous cobalt oxide, hydrous nickel oxide, and basic

Received: September 13, 2010
Revised: January 9, 2011
Published: January 31, 2011

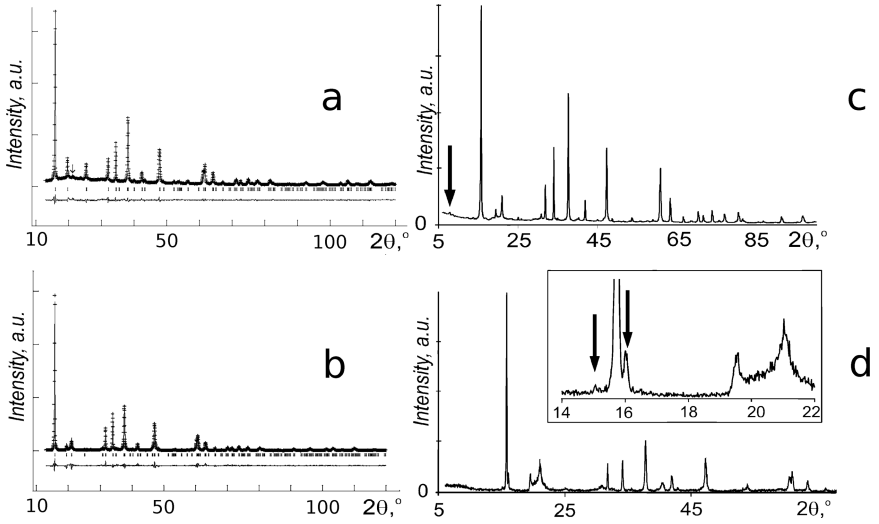

Figure 1. X-ray diffraction patterns of $Na_2Ni_2TeO_6$ (a), $Na_2Zn_2TeO_6$ (b), $Na_2Co_2TeO_6$ (c), and $Na_2Mg_2TeO_6$ (d). (a,b): crosses, experimental data; line, calculated profile; bottom, difference; vertical bars, Bragg positions. An arrow points to the 101 reflection, not permitted by $P6_3/mcm$ space group.(c): Arrow points to the 001 reflection, forbidden by $P6_322$ space group. (d): Arrows indicate impurity peaks.

carbonates of zinc and magnesium. The first three substances were dried at 200 °C and stored in a desiccator, and the remaining four were analyzed for volatile components by weight loss on calcination and then used in their air-dry form. The reagents were mixed in desired ratios with a mortar and pestle, pressed, and calcined: first at 600−650 °C for 2−10 h to expel volatile components and oxidize Te(4+) to Te(6+), and then at 800−820 °C for 2−4 h, with intermediate regrinding and pressing, to achieve homogeneity. Of the two sodium sources, the nitrate is favorable because of its low melting point and ability to oxidize Te(4+) with no need for diffusion of the atmospheric oxygen into the pressed pellet. On the other hand, large amounts of the liquid might cause macroscopic inhomogeneity due to liquation. Thus, we usually introduced 80% of the desired Na as carbonate and only 20% as nitrate.

Ceramic samples for conductivity measurements were prepared by the uniaxial hot pressing at 800 °C and 30 MPa. A green cylindrical compact was surrounded by coarse-grained alumina. After the hot pressing, the contaminated outer layers were eliminated and rectangular samples [typically (3−5 mm) × 7 mm × 8 mm] were cut with a diamond saw. Their weights and dimensions were measured carefully and used to calculate apparent densities as percentages of the corresponding X-ray densities. Opposite sides of a sample were electroded with molten indium, and its immittance was measured in the frequency range of 20 Hz to 200 kHz with an original immittance analyzer developed in the Institute of Control Sciences, Russian Academy of Sciences. The accuracy of the instrument was verified against standard resistors and capacitors. The measurements were made in air at several stabilized temperatures between 20 and 350−400 °C in heating/cooling cycles to verify repeatability. Electronic contribution to the total conductivity was estimated by the dc polarization method using voltages of 100−200 mV, i.e., far below possible decomposition voltages of the solid electrolytes.

The X-ray phase analysis of powders and ceramics and also texture studies were performed with a DRON-2.0 diffractometer using Ni-filtered CuKα radiation. Higher-quality patterns for structural studies were taken employing a Rigaku D/Max-RC instrument with a rotating Cu anode and a secondary beam graphite monochromator; amorphous powders (coffee, beryllium hydroxide, or beryllium carbonate) were admixed to reduce grain orientation effect. For the high-temperature study, an ARL X'TRA diffractometer was used, equipped with a TTK 450 camera (Anton Paar) and an energy-dispersive Si(Li) detector, also with CuKα radiation. Room-temperature lattice constants were refined by Celref 3 (Laugier and Bochu, 2001) using corundum powder (NIST SRM 676) as an internal standard assuming $a = 4.7592$ Å and $c = 12.9920$ Å. For Rietveld refinements, the GSAS+EXPGUI suite[24,25] was used.

Although oxidation states of Te, Ni, and Co were evident from the structural results, they were further verified by redox titration. Weighed samples of the tellurates were dissolved on heating in aliquots of the aqueous solution containing 2 mol/L H_2SO_4 and 0.1 mol/L $FeSO_4$, converting Te(6+) to Te(4+) and M(3+) (if any) to M(2+). The resulting solutions were cooled and titrated with a standard $KMnO_4$ solution, oxidizing Te(4+) back to Te(6+) and excess Fe(2+) to Fe(3+). All the procedures were repeated with identical aliquots where no tellurate was added. Any difference between the volumes of the permanganate solution would indicate a deviation from the expected oxidation states of M(2+) and Te(6+).

3. RESULTS AND DISCUSSION

3.1. Phase Analysis and Chemical Compositions. In the systems $Na_xM^{2+}_{(2+x)/4}Te^{6+}_{(2-x)/4}O_2$ (M = Ni, Zn), in contrast to previously studied $Na_xCr^{3+}_xTi^{4+}_{1-x}O_2$,[12] $Na_xM^{2+}_{x/2}Ti^{4+}_{1-x/2}O_2$ (M = Co, Ni),[10,11] $Na_xLi^{+}_{x/3}Ti^{4+}_{1-x/3}O_2$[13] etc., homogeneous P2-type phases were only found at $x = 2/3$ (Figure 1a,b). When x deviated from this value, additional phases appeared, which will be described elsewhere. This means that Te^{6+}/M^{2+} substitution is hardly possible, and the tripled formulas, $Na_2M_2TeO_6$, are more correct. Then, with M = Co and Mg, only these compositions were prepared (Figure 1c,d). Unfortunately, the Mg compound could not be obtained as a single phase because of kinetic hindrances and always showed weak reflections from unknown impurities, marked with arrows in Figure 1d. Because of the known volatility of tellurium oxides, we avoided the very high temperatures necessary to achieve equilibrium in the Mg system.

Redox titrations confirmed oxygen content of 5.99−6.03 (±0.03) in the Ni, Co, and Zn compounds. Strictly speaking, the chemical analysis cannot distinguish between $Na_2M^{2+}{}_2Te^{6+}O_6$ and $Na_2M^{3+}{}_2Te^{4+}O_6$, but the latter formula is chemically improbable and does not conform with the observed bond lengths (see below).

It is obvious that the main obstacle for M^{2+}/Te^{6+} substitutional disorder is their great difference in oxidation numbers.

dx.doi.org/10.1021/cm102629g |*Chem. Mater.* 2011, 23, 1174–1181

Table 1. Hexagonal Lattice Parameters and Colors of New Tellurates in Comparison with the Literature Data for the Co Compound[a]

	color	$^{VI}R(M^{2+})$ (Å)	a (Å)	c (Å)	c/a (Å)	V (Å^3)
$Na_2Ni_2TeO_6$	light green	0.83	5.2042(5)	11.1383(5)	2.140	261.3
$Na_{2.1}Ni_{1.9}Li_{0.1}TeO_6$	light green		5.2100(7)	11.1763(1)	2.145	262.7
$Na_{1,9}Ni_{1,9}Fe_{0,1}TeO_6$	yellow		5.2044(10)	11.2261(3)	2.157	263.3
$Na_2Mg_2TeO_6$	white	0.86	5.2538 (14)	11.2603 (2)	2.143	269.2
$Na_2Zn_2TeO_6$	white	0.88	5.2784(6)	11.2895(1)	2.139	272.4
same at 300 °C			5.2950(7)	11.3505(1)	2.144	275.6
expansion coeff. (K^{-1})			1.1×10^{-5}	2.0×10^{-5}		4.3×10^{-5}
$Na_2Co_2TeO_6$	pink	0.885 (HS)	5.2727(5)	11.2301(1)	2.130	270.4
$Na_2Co_2TeO_6$[23]	light pastel		5.2889(1)	11.2149(4)	2.120	271.7

[a] Thermal expansion coefficients are also listed for the Zn compound.

Table 2. Crystallographic Data, Details of Data Collection, and Structure Refinement of $Na_2M_2TeO_6$ (M = Ni, Zn)

M	Ni	Zn
space group	$P6_3/mcm$ (No.193)	$P6_322$ (No.182)
lattice constant: a (Å)	5.2074(1)	5.2796(2)
lattice constant: c (Å)	11.1558(4)	11.2941(4)
cell volume (Å^3)	261.98	272.64
formula weight	387.0	400.3
Z	2	2
tube voltage (kV)	55	55
tube current (mA)	180	180
2θ range	12.5−120°	10−120°
step size (deg)	0.02	0.02
count time (s)	2	1
number of data points	5374	5500
number of reflections	172	220
number of parameters	34	39
agreement factors R_p	4.44%	5.15%
R_{wp}	5.25%	6.03%
χ^2	1.86	2.23

Table 3. Atomic Coordinates, Occupancies, and Thermal Displacement Parameters for $Na_2Ni_2TeO_6$ and $Na_2Zn_2TeO_6$

space group		x	y	z	s.o.f.	U_{iso}
$P6_3/mcm$	Te	0	0	0	1	0.00274(9)
	Ni	2/3	1/3	0	1	0.00010(5)
	O	0.6729(5)	0.6729(5)	0.5927(4)	1	0.00005(4)
	Na1	0.3495(7)	0	1/4	0.438(4)	0.01684(9)
	Na2	1/3	2/3	1/4	0.207(2)	0.00151(3)
	Na3	0	0	1/4	0.245(2)	0.07088(9)
$P6_322$	Te	1/3	2/3	1/4	1	0.0067(5)
	Zn1	0	0	1/4	1	0.0001(1)
	Zn2	1/3	2/3	3/4	1	0.010(5)
	O	0.3594(10)	0.3312(11)	0.6501(6)	1	0.0001(1)
	Na1	0.6615(11)	0	0	0.280(7)	0.0001(1)
	Na2	0	0	0	0.043(5)	0.0001(1)
	Na3	1/3	2/3	0.5111(9)	0.535(9)	0.0029(9)

With a slightly lower difference of 3, disordered arrangement was observed for Cr^{3+}/Te^{6+} in the pyrochlore structure,[26] for Li^+/Ti^{4+} and M^{2+}/Sb^{5+} in the P2-type (see above), whereas in the structurally related O3-type, both ordered and disordered arrangements of Li^+/Ti^{4+} and M^{2+}/Sb^{5+} were observed, depending on their atomic ratio.[13,27] Note that the ionic radii[28] difference for ordered Ni^{2+}/Te^{6+} (0.13 Å) is slightly lower than those for disordered Co^{2+}/Sb^{5+} (0.145 Å) and Li^+/Ti^{4+} (0.155 Å). On the other hand, slightly greater radii differences of 0.16−0.19 Å results in Ni^{2+}/Mn^{4+} and Mg^{2+}/Mn^{4+} ordering in Na_2M^{2+}-Mn_2O_6[6], although the difference in the oxidation numbers is only 2.

3.2. Crystal Structures. X-ray powder patterns of all the four compounds (Figure 1a−d) are similar to those of the above-mentioned titanates, and most reflections may be indexed on small $P6_3/mmc$ cells with a = 3.00−3.04 and c = 11.14−11.31 Å. However, there are also superlattice reflections which need $a(3)^{1/2} \times a(3)^{1/2} \times c$ cells with tripled volumes, in accordance with the tripled formula units (Table 1). For $Na_2Ni_2TeO_6$, the superlattice reflections with index l odd are very weak, and only two of them were observed, with I < 1%, in contrast to 15 superlattice reflections with l even, with intensities up to 10%. This means that the heavy atoms are arranged with a repeat distance of c/2, i.e., Te above Te and Ni above Ni. The highest symmetry space group accounting for this feature and preserving the P2-type $P6_3/mmc$ subcell is $P6_3/mcm$. Refinement in this group rapidly converged to a suitable result with low R-factors and χ^2 and reasonable bond lengths (Tables 2, 3, and 4).

For the three other compounds (M = Co, Zn, Mg), the situation with superlattice reflections is reversed: those having l odd are much stronger than those with l even (Figure 2). This means that arrangement of the heavy atoms does not have a repeat of c/2, i.e., M and Te alternate along the c axis. Because there are unequal amounts of M and Te, there should also be columns solely occupied by M. This is best described by $P6_322$ space group, and $Na_2Zn_2TeO_6$ was successfully refined in this group (Tables 2, 3, and 4). The same model was found for $Na_2Co_2TeO_6$ in the parallel study.[23] Both models are illustrated in Figure 3.

It should be noted that both neutron[23] and X-ray diffraction patterns of $Na_2Co_2TeO_6$ exhibit a very weak reflection at d ≈ 11 Å, corresponding to 001, forbidden in $P6_322$, and similar but even weaker reflection is also observed for the Zn compound, whereas the Ni compound shows a very weak 101 reflection, forbidden in $P6_3/mcm$. In addition, the Zn compound has several extremely weak reflections, which only can be indexed on a primitive orthorhombic supercell with a = 5.2701(5), b = 9.1439(8), and c = 11.2896(9) Å, although no line splitting is observed

dx.doi.org/10.1021/cm102629g |Chem. Mater. 2011, 23, 1174–1181

Table 4. Principal Interatomic Distances (Å) in $Na_2M_2TeO_6$ (M = Ni, Zn)

M	Ni		Zn
Te−O	1.993(3) × 6		1.971(6) × 6
sum of radii[28]		1.95	
M1−O	2.035(5) × 6		2.148(5) × 6
M2−O	−		2.162(6) × 6
sum of radii[28]	2.08		2.13
Na1−O	2.432(8) × 2		2.383(8) × 2
	2.489(5) × 4		2.398(6) × 2
			2.559(6) × 2
average	2.47		2.45
sum of radii[28]		2.41	
Na2−O	2.480(4) × 6		2.493(5) × 6
Na2−M	2.7889(1) × 2		2.8235(1) × 2
Na3−O	2.446(4) × 6		2.422(9) × 3
			2.435(10) × 3
average			2.429
Na3−M	−		2.698(10)
Na3−Te	2.7889(1) × 2		2.949(10)

because $b/a = 1.735$ is very close to $3^{1/2}$. Almost all these reflections vanish at 300 °C but appear again on cooling (Figure 4). These subtle effects (possibly, due to Na/vacancy ordering and/or an admixture of the $P6_322$ polytype in the Ni compound) could not be properly accounted for in the profile refinements and have been ignored both here and in the parallel study.[23] Because our observed intensities for $Na_2Co_2TeO_6$ agreed with the published structural data,[23] we did not attempt a rerefinement.

Lattice parameters in Table 1 have been refined using peak positions measured with the internal standard, whereas those in Table 2 are from full-profile refinements; this explains slight systematic differences between the two data sets: 0.02−0.04% for M = Zn and 0.06−0.16% for M = Ni.

However, there are small but not negligible differences in lattice parameters for the Co compound from the two sources (Table 1), which cannot be explained by systematic errors because our *c* axis is 0.14% longer but our *a* axis is 0.31% shorter. These deviations are typical of the cases where *x* is decreased: a smaller radius of a higher-valence octahedral cation produces contraction in the ab plane, whereas sodium deficiency in the interlayer space produces *c*-axis expansion.[10−13] Viciu et al.[23] prepared $Na_2Co_2TeO_6$ in nitrogen from Co_3O_4 and TeO_2 with 20% excess Na_2CO_3 (to compensate for volatilization during 8 days at 800 °C), but our preparations were made in air with no excess Na_2CO_3. Hence, there may be two explanations for the observed differences. First, oxygen excess in Co_3O_4 was insufficient for complete oxidation of TeO_2 to Te(6+), and thus, there might be a small admixture of Te(4+) or TeO_2 volatilization and small Co substitution for Te, both effects accompanied with excess Na to attain electroneutrality. Second, partial oxidation might take place in our preparation to give $Na_{2-y}Co^{2+}{}_{2-y}Co^{3+}{}_yTeO_6$. According to Shannon's radii,[28] bond lengths $HSCo^{2+}-O^{2-}$ and $LSCo^{3+}-O^{2-}$ differ by 10%. Thus, a very small percentage of LS (low-spin) Co^{3+} may cause a noticeable change in lattice parameters. It is worth noting that no such difference in lattice parameters was observed with $Na_3Co_2SbO_6$ prepared in nitrogen[23] and air.[27]

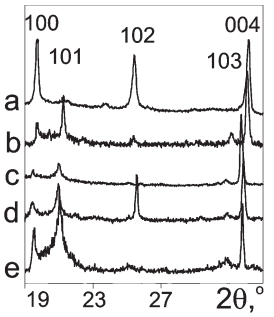

Figure 2. Comparison of X-ray diffraction patterns in the region where strongest superlattice reflections are observed: (a) $Na_2Ni_2TeO_6$, (b) $Na_{2.1}Ni_{1.9}Li_{0.1}TeO_6$, (c) $Na_2Zn_2TeO_6$, (d) $Na_2Co_2TeO_6$, and (e) $Na_2Mg_2TeO_6$.

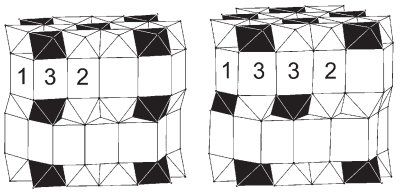

Figure 3. Comparison of crystal structures of $Na_2Ni_2TeO_6$ (left) and $Na_2M_2TeO_6$ (M = Zn, Co, Mg) (right). Black octahedra, TeO_6; white octahedra, MO_6 (M = Ni, Zn, Co, Mg); and prisms, NaO_6.

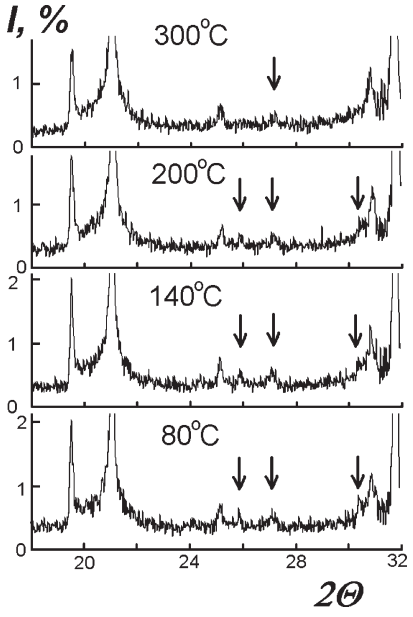

Figure 4. Fragments of the X-ray patterns of $Na_2Zn_2TeO_6$ at elevated temperatures. The patterns have been taken in the following sequence (top to bottom): 300, 200, 140, and 80 °C. Arrows point to the three strongest reflections, which only could be indexed with an orthorhombic supercell.

The same two superstructure types were found for $Na_2MMn_2O_6$,[6] but the role of M cations was exactly opposite: M = Mg gave rise to the $P6_3/mcm$ superstructure, whereas the superstructure with M = Ni, although not refined completely, was better described by the $P6_322$ model. Factors affecting formation of one variant or other are not clear yet. We only can notice that

dx.doi.org/10.1021/cm102629g |*Chem. Mater.* 2011, 23, 1174–1181

Table 5. Percentage of Sodium Occupying Various Trigonal Prism Types in $Na_2M_2TeO_6$[a]

number	prism type	M = Ni	M = Zn	M = Co[23]
1	sharing edges with two TeO_6 and four MO_6 octahedra and rectangular faces with two prisms 2 and one prism 3	67	43	70
2	sharing faces with two MO_6 octahedra and three prisms 1	21	2	6
3	sharing faces with two TeO_6 octahedra and three prisms 1	12	–	–
3	sharing faces with one TeO_6, one MO_6 and three prisms 1	–	55	24

[a] For the Co compound, prism numbering in this table is different from that in ref 23 (1 and 3 interchanged).

Ni^{2+} has the smallest ionic radius and the highest electronegativity among the four M^{2+} cations under study, but no direct relation could be found between these characteristics and stacking mode. It is evident, however, that both types are almost equivalent energetically. Actually, we have found that just 5% Li substitution for Ni ($Na_{2.1}Ni_{1.9}Li_{0.1}TeO_6$) converts the Ni compound from $P6_3/mcm$ to $P6_322$ (Figure 2). Note that Li^+ is larger than Ni^{2+}, whereas Fe^{3+} is smaller, and similar substitution with Fe^{3+} ($Na_{1.9}Ni_{1.9}Fe_{0.1}TeO_6$) does not induce rearrangement to $P6_322$.

The most interesting structural question is the distribution of sodium ions over the interlayer prisms. It seems to be disordered in spite of M/Te ordering. In the P2-aristotype, there are equal amounts of prisms 1, sharing their triangular bases with empty tetrahedra, and prisms 2, sharing their bases with occupied octahedra. A significant portion of the mobile cations is usually accumulated in prisms 2,[4,6,9,13,14] in apparent contradiction with the Pauling's Third Rule (face sharing should be avoided). This was explained by the repulsion between the mobile ions, which tends to maximize distances between them.[13,14] Another manifestation of this repulsion is the shift of the sodium cations from the centers of their prisms found by neutron diffraction first in mixed titanates[14] and then in Na_xCoO_2[4] and $Na_2Co_2TeO_6$,[23] although some Na−O distances in $Na_2Co_2TeO_6$ (2.13 and 2.19 Å) seem to be unrealistically short.

Off-center sodium displacements might be expected in this work, too. However, they could not be confirmed definitely due to the low X-ray scattering factor of Na^+, and site splitting was not attempted. Nevertheless, independent refinements of the nonequivalent prism occupancies resulted in the total sodium contents very close to the nominal value of 4 per unit cell: 3.94 for the Ni compound and 3.91 for the Zn compound. These somewhat reduced values, together with high thermal parameters of the sodium ions, are obviously due to high sodium mobility (see below) and possible static off-center displacements.

In the ordered P2 derivatives, prisms 2 are further split into two types, differing by the nature of cations in the neighboring octahedra. Taking into account only the first coordination sphere (six oxygens), all three prism types in both structure types are practically equivalent. The quadrangular faces of the prisms are strictly planar and orthogonal in the $P6_3/mcm$ structure and slightly distorted in the Zn and Co compound, their torsion angles being only 3−4° and 7−8° in both compounds. The second coordination spheres and occupancies of sodium prisms are characterized in Table 5. The most surprising result is that in both Co and Zn compounds the prism 3 neighboring with one Te^{6+} and one M^{2+} ion has essentially greater occupancy than prism 2 neighboring with two M^{2+}. The reasons for this may be still unknown details of local Na/vacancy order and/or influence of the next polyvalent neighbors. For example, in the Zn compound, Na2 is surrounded by $6Te^{6+}$ and $6Zn^{2+}$ at a distance of 4.15 Å, whereas Na3 has only $3Te^{6+}$ and $3Zn^{2+}$ at a distance of 4.07 Å and also $6Zn^{2+}$ at a distance of 4.24 Å, and this may give some preference to site 3.

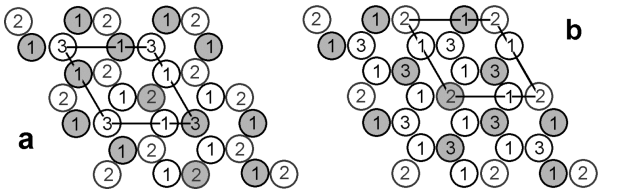

Figure 5. Sodium plane in $Na_2Ni_2TeO_6$ (a) and $Na_2Zn_2TeO_6$ (b). Filled and empty circles show possible momentary arrangements of occupied and empty sites.

Table 6. Bottleneck Radii (Å) for Sodium Transport in $Na_2M_2TeO_6$[a]

Path	Na1−Na2	Na1−Na3
M = Ni	2.32	2.29
M = Zn	2.28	2.29
M = Co	2.31	2.32

[a] For the Co compound, site numbering in this table is the same as in Table 6 and different from that in the original paper.[23].

Figure 5 shows arrangements of the partially occupied sodium sites in both structure types and also some possible momentary arrangements of sodium ions. Almost all sodium sites have an asymmetrical sodium environment with distances to the nearest sodium neighbors of 2.94−3.10 and 3.49−3.54 Å [$\approx a/(3)^{1/2}$ and $\approx 2a/3$, respectively]. Because of the asymmetrical Na^+−Na^+ repulsion, the cations should displace from the ideal positions indicated in Table 3 and Figure 5, as discussed above, and the real Na^+−Na^+ distances should become even larger.

As evident from Figure 5, partially occupied sodium sites in both structure types form a 2-D continuous net of diffusion paths with very short intersite distances of 1.70−1.82 Å (whereas actual Na−Na distances are much greater as discussed above). Together with wide quadrangular bottlenecks between the prisms (Table 6), this is a prerequisite for high sodium ion conductivity. The terms "bottleneck size" and "bottleneck diameter" may have different meanings, and some authors base them on undefined ionic radii. To avoid ambiguity, we shall try to give a strict definition. Here, bottleneck radius is the smallest of the maximin Na−O distances on Na^+ diffusion path, i.e., Na−O distance in the narrowest place of the path. Generally, the bottleneck is defined by three ions; the coordination number of a mobile ion in a bottleneck may be larger (four or six) only in specific most symmetrical cases. In the $P6_3/mcm$ structure, it is four, and in the $P6_322$ structures, it is 3 + 1, because the fourth distance is only slightly larger than other three.

Figure 5 shows that the paths remain continuous, even if we exclude the least populated sites: Na3 in the Ni compound and

Na2 in the Zn and Co compounds. In addition, Table 6 demonstrates that the bottlenecks leading to these least populated sites (only surrounded by Na1) are somewhat narrower than those on the main continuous paths. Therefore, these sites may be excluded from the consideration of fast ionic transport, and only the widest bottlenecks in each compound are important, their radii being 2.32 Å in the Ni and Co compounds and 2.29 Å in the Zn compound.

3.3. Ionic Conductivity. The conductivity has been measured using hot-pressed samples. With layered structures, the uniaxial hot pressing might produce grain orientation and, thus, anisotropic conductivity.[10,29] To examine this possibility, X-ray patterns have been taken from the perpendicular faces of the same rectangular samples, as shown in Figure 6. We selected a pair of reflections, 0 0 4 and 1 1 0, which are most informative because they result from planes perpendicular and parallel to the principal crystallographic axis and have similar Bragg angles. Comparison of their intensities (Figure 6) shows a small degree of grain orientation in the Ni and Zn compounds and absence of the effect in the Co compound, obviously due to great amounts of surrounding alumina grains, which provided a quasi-hydrostatic regime, and also to relatively mild hot-pressing conditions because temperatures in the excess of 800 °C were avoided. On the basis of these results, the conductivity was measured parallel to the longest dimension of a rectangular sample, i.e., perpendicular to the pressure direction, to provide greater sample resistance and, thus, lower contribution from other factors such as quality of contacts and uncertainty in interpretation of the immittance diagrams. The mild hot-pressing conditions are also responsible for the relatively low densities of the ceramics (Table 7).

Impedance diagrams of the ceramic samples are typical of ionic conductors with blocking electrodes. Two examples are shown in Figure 7. At low temperatures, they contain a low-frequency electrode response in the form of an inclined straight line characteristic of a constant phase element (CPE) and a truncated high-frequency arc characteristic of a parallel connection of the sample resistance and geometric capacity. At elevated temperatures, only the CPE response is visible because the arc is beyond the available frequency range. The sample resistance is obtained as the intercept of the straight line with the real axis and, thus, may include not only bulk resistance but also a contribution from the grain boundary resistance.

Panels a−e of Figure 8 illustrate temperature dependences of the conductivities and also reproducibility of the data. Panel a of Figure 8 shows that heating/cooling repeatability is satisfactory, but data for two nominally identical $Na_2Ni_2TeO_6$ samples agree only at elevated temperatures. Discrepancies in the vicinity of the room temperature are obviously due to different contributions from grain boundary resistances and minor impurity phases

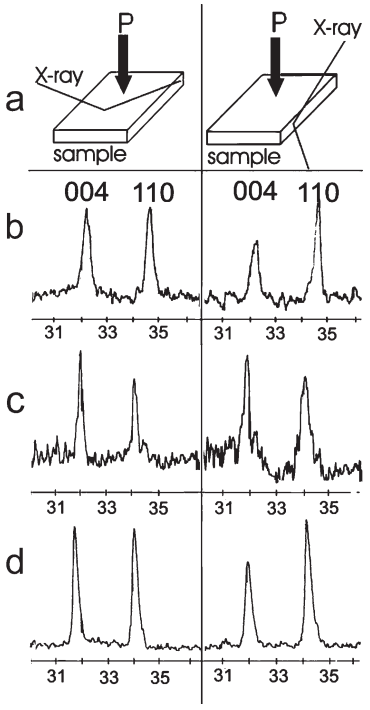

Figure 6. (a) Schematic of the sample orientation with respect to the hot-pressure axis and X-ray beams during texture examination. (b−d) Comparison of X-ray reflections from the two perpendicular faces of the $Na_2M_2TeO_6$ samples, M = Ni (b), Co (c), and Zn (d).

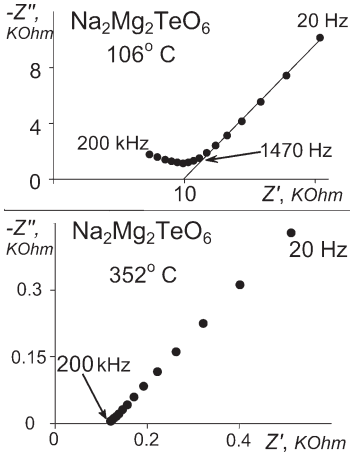

Figure 7. Typical impedance plots of the ceramic samples.

Table 7. Ionic Conductivities (σ) and Activation Energies (E_a) for Polycrystalline Samples of Layered Tellurates

formula	density (% theor.)	σ (S m^{-1}) 25 °C	σ (S m^{-1}) 300 °C	E_a (kJ/mol) (100−350 °C)
$Na_2Ni_2TeO_6$	79.6 − 80.3	0.0008 − 0.0034	10.1−10.8	53.4
$Na_{1.9}Ni_{1.9}Fe_{0.1}TeO_6$	72	0.01	4.7	36.8
$Na_2Zn_2TeO_6$	55−68	0.009	5.1− 7.0	−
$Na_2Co_2TeO_6$	56−82	$(3.8−4.9) \times 10^{-4}$	3.1−4.4	50.6
$Na_2Mg_2TeO_6$	74	0.0063	2.3	−

dx.doi.org/10.1021/cm102629g |*Chem. Mater.* 2011, 23, 1174–1181

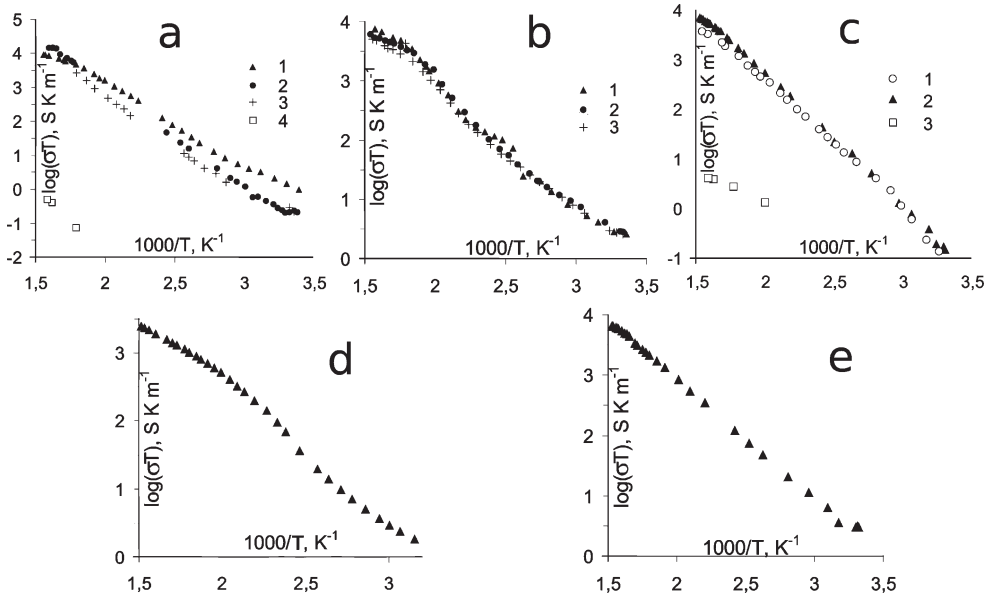

Figure 8. Arrhenius plots for total (ac) conductivity (unless otherwise stated). (a) $Na_2Ni_2TeO_6$: (1) sample 1, heating; (2)/(3) sample 2, heating/cooling; (4) sample 2, electronic (dc) conductivity, heating. (b) $Na_2Zn_2TeO_6$: three different samples. (c) $Na_2Co_2TeO_6$: (1), (2) two different samples; (3) dc data (electronic conductivity). (d) $Na_2Mg_2TeO_6$. (e) $Na_{1.9}Ni_{1.9}Fe_{0.1}TeO_6$.

(beyond detection limit of the XRD and probably glass-like). For the Zn and Co compounds, reproducibility is better (Figure 8b,c).

Conductivities and their activation energies of the four compounds are compared in Table 7. Unambiguous explanation of the data is complicated because it is difficult to separate intrinsic (crystal-chemistry) effects from the technological factors resulting in variations in density, grain orientation, and possible presence of glassy admixtures. Thus, only tentative explanations may be given.

At elevated temperatures, $Na_2Ni_2TeO_6$ samples exhibit highest conductivities, in agreement with the widest bottleneck, relatively high ceramic density, grain orientation effect, and highest electronegativity[30] of Ni (as compared with Co, Zn, and Mg), which favors higher ionicity of O−Na bonds. Surprisingly, the room-temperature conductivity of the Ni compound is lower than those of most other samples (despite considerable amount of crystalline impurities in the Mg sample). We suppose that this might be due to a minor admixture of a glassy phase (which might be also responsible for better sinterability) in the $Na_2Ni_2TeO_6$ samples. Low conductivity of the glass should be associated with high activation energy, and thus, its detrimental effect should be less significant at elevated temperatures.

Despite the relatively low density, the conductivities of all the three compounds with M = Co, Ni, and Zn, together with the Fe-doped sample (Figure 8e) are surprisingly high, in the range of 4−11 S/m at 300 °C, and compare well with those for dense ceramics of the disordered P2-type titanates[10−12] and β-alumina.[31] Equally surprising is the relatively high conductivity of the Mg-based sample (Figure 8d), despite the considerable amount of foreign phase(s). By analogy with the known layered materials,[10] it may be expected that dense single-phase grain-oriented ceramics, as it is prepared, should have 2−4 times greater conductivity.

Plots in panels b and d of Figure 8 deviate from linearity, i.e., disobey the Arrhenius law. This might be due to phase transitions. To examine this possibility, we performed a high-temperature XRD study of $Na_2Zn_2TeO_6$, but no distinct phase transition could be detected. Between 25 and 300 °C, the (pseudo)hexagonal lattice remains essentially the same, with reasonable thermal expansion coefficients (TECs) listed in Table 1. As might be expected, the TEC for the direction perpendicular to the layers is much larger than that for the in-plane direction. The only observed change (Figure 4) was the reversible disappearance of some (but not all!) extremely weak (<0.4%) reflections forbidden in the space group $P6_322$ and demanding orthorhombic primitive cell as reported in Section 3.2. This effect correlates with the change of slope of the Arrhenius plot observed between about 220 and 260 °C in panel b of Figure 8 and may be due to some subtle changes in the sodium arrangement ignored in the $P6_322$ model.

For the cations with partially filled d shells (Co and Ni), oxidation states may vary, giving rise to electronic conductivity. However, our polarization measurements showed that the electronic contribution is only 0.1% at 300 °C for the Co compound (Figure 8c) and much lower for the Ni compound (Figure 8a) making them essentially pure ionic conductors.

CONCLUSIONS

A new group of solid electrolytes, $Na_2M_2TeO_6$ (M = Ni, Zn, Co, Mg), have been found and characterized by X-ray profile refinement, redox titration, impedance, and dc polarization measurements. They represent two different superstructures of the known layered P2-type and, despite complete ordering of the M^{2+} and Te^{6+} in the rigid lattice, have an apparently disordered sodium arrangement and high sodium ion conductivity. This opens the way to new ordered P2-type solid electrolytes, possibly with more redox-stable and cheap components. To elucidate sodium order/disorder behavior, a neutron diffraction study is desirable.

ASSOCIATED CONTENT

Supporting Information. X-ray crystallographic files (CIFs). This material is available free of charge via the Internet at http://pubs.acs.org.

AUTHOR INFORMATION

Corresponding Author
*E-mail: maevstigneeva@gmail.com.

ACKNOWLEDGMENT

The work was supported by the Internal Grant K-07-T-20 of the Southern Federal University and by Grant-in-Aid 00-15 from the International Centre for Diffraction Data. The authors are also thankful to Dr. S.N. Polyakov for his help with the D/Max scans.

REFERENCES

(1) Terasaki, I.; Sasago, Y.; Uchinokura, K. *Phys. Rev.* **1997**, *B 56*, R12685.
(2) Lee, M.; Viciu, L.; Li, L.; Wang, Y.; Foo, M. L.; Watauchi, S.; Pascal, R. A., Jr.; Cava, R. J.; Ong, N. P. *Nat. Mater.* **2006**, *5*, 537–540.
(3) Takada, K.; Sakurai, H.; Takayama-Muromachi, E.; Izumi, F.; Dilanian, R. A.; Sasaki, T. *Nature* **2003**, *422*, 53–55.
(4) Jorgensen, J. D.; Avdeev, M.; Hinks, D. G.; Burley, J. C.; Short, S. *Phys. Rev.* **2003**, *B 68*, 214517.
(5) Delmas, C.; Braconnier, J.-J.; Hagenmuller, P. *Mater. Res. Bull.* **1982**, *17*, 117–123.
(6) Paulsen, J. M.; Donaberger, R. A.; Dahn, J. R. *Chem. Mater.* **2000**, *12*, 2257–2267.
(7) Delmas, C.; Fouassier, C.; Reau, J.-M.; Hagenmuller, P. *Mater. Res. Bull.* **1976**, *11*, 1081–1086.
(8) Maazaz, A.; Delmas, C.; Fouassier, C.; Reau, J.-M.; Hagenmuller, P. *Mater. Res. Bull.* **1979**, *14*, 193–199.
(9) Smirnova, O. A.; Nalbandyan, V. B.; Avdeev, M.; Medvedeva, L. I.; Medvedev, B. S.; Kharton, V. V.; Marques, F. M. B. *J. Solid State Chem.* **2005**, *178*, 172–179.
(10) Nalbandyan, V. B.; Shukaev, I. L. *Russ. J. Inorg. Chem. (Engl. Transl.)* **1992**, *37*, 1231–1235. *Zh. Neorg. Khim.*, **1992**, *37*, 2387-2394.
(11) Shukaev, I. L.; Volochaev, V. A. *Russ. J. Inorg. Chem. (Engl. Transl.)* **1995**, *40*, 1974–1980. *Zh. Neorg. Khim.* **1995**, *40*, 2056-2062.
(12) Avdeev, M.Yu.; Nalbandyan, V. B.; Medvedev, B. S. *Inorg. Mater. (Engl. Transl.)* **1997**, *33*, 500–503. *Neorg. Mater.* **1997**, *33*, 595-599.
(13) Shilov, G. V.; Nalbandyan, V. B.; Volochaev, V. A.; Atovmyan, L. O. *Int. J. Inorg. Mater.* **2000**, *2*, 443–449.
(14) Avdeev, M.Yu.; Nalbandyan, V. B.; Beskrovnyi, A. I. In , 6th European Powder Diffraction Conference (EPDIC-6), Budapest, Hungary, August 22−25, 1998, p 235.
(15) Zandbergen, H. W.; Foo, M. L.; Xu, Q.; Kumar, V; Cava, R. J. *Phys. Rev. B* **2004**, *70*, 024101.
(16) Yang, H. X.; Nie, C. J.; Shi, Y. G.; Yu, H. C.; Ding, S.; Liu, Y. L.; Wu, D.; Wang, N. L.; Li, J. Q. *Solid State Commun.* **2005**, *134*, 403–408.
(17) Roger, M.; Morris, D. J. P.; Tennant, D. A.; Gutmann, M. J.; Goff, J. P.; Hoffmann, J.-U.; Feyerherm, R.; Dudzik, E.; Prabhakaran, D.; Boothroyd, A. T.; Shannon, N.; Lake, B.; Deen, P. P. *Nature* **2007**, *445*, 631–634.
(18) Shu, G. J.; Chou, F. C. *Phys. Rev. B* **2008**, *78*, 052101.
(19) Blangero, M.; Decourt, R.; Carlier, D.; Ceder, D.; Pollet, M.; Doumerc, J.-P.; Darriet, J.; Delmas, C. *Inorg. Chem.* **2005**, *44*, 9299–9304.
(20) Xu, J.; Assoud, A.; Soheilnia, N.; Derakhshan, S.; Cuthbert, H. L.; Greedan, J. E.; Whangbo, M. H.; Kleinke, H. *Inorg. Chem.* **2005**, *44*, 5042–5046.
(21) Petrenko, A. A.; Nalbandyan, V. B.; Pospelov, A. A.; Politaev, V. V.; Evstigneeva, M. A.; Serikova, E. I.; Kataev, A. A.; Shukaev, I. L. In , XIII International Chugaev Conference on Coordination Chemistry, Odessa, Ukraine, September 4−7, 2007, p 549 (in Russian).
(22) Nalbandyan, V. B.; Evstigneeva, M. A.; Petrenko, A. A.; Medvedev, B. S.; Ni, E. V. In . International Scientific Workshop, June 22−26, 2009, Lviv, Ukraine, 2009, p 72. http://ena.lp.edu.ua:8080/handle/ntb/5621.
(23) Viciu, L; Huang, Q.; Morosan, E.; Zandbergen, H. W.; Greenbaum, N. I.; McQueen, T.; Cava, R. J. *J. Solid State Chem.* **2007**, *180*, 1060–1067.
(24) Larson, A. C.; Von Dreele, R. B. ; LAUR 86-748; Los Alamos National Laboratory, Los Alamos, NM, 2004.
(25) Toby, B. H. *J. Appl. Crystallogr.* **2001**, *34*, 210–213.
(26) Isasi, J; Lypez, M. L.; Veiga, M. L.; Pico, C. *Solid State Ionics* **1996**, *89*, 321–326.
(27) Politaev, V. V.; Nalbandyan, V. B.; Petrenko, A. A.; Shukaev, I. L.; Volotchaev, V. A.; Medvedev, B. S. *J. Solid State Chem.* **2010**, *183*, 684–691.
(28) Shannon, R. D. *Acta Crystallogr.* **1976**, *A32*, 751–767.
(29) Nalbandyan, V. B. *Inorg. Mater. (Engl. Transl.)* **1991**, *27*, 838–842. *Neorg. Mater.* **1991**, *27*, 1006−1010.
(30) Emsley, J. *The Elements*; Clarendon Press: Oxford, 1991 (Russian translation; Mir: Moscow, 1993).
(31) Sudworth, J. L.; Tilley, A. R. *The Sodium−Sulphur Battery*; Chapman and Hall: London, 1985 (Russian translation; Mir: Moscow, 1988).